BASIC ORBIT PROPERTIES OF IONS IN A MIGMA FUSION DEVICE*

M. M. GORDON and D. A. JOHNSON

Cyclotron Laboratory, Physics Department, Michigan State University, East Lansing. Michigan 48824, U.S.A.

The "Migma Cell" designed by Maglich is aimed at producing useful fusion power by storing deuterons in precessing, self-colliding orbits in a suitable magnetic field[1]). We have undertaken a more thorough analysis of the basic orbit properties in such a device. Using equilibrium orbit and transfer matrix techniques, we have developed a computer code which calculates all the important properties of median plane orbits and of vertical focusing in the given magnetic field as a function of momentum.

The results obtained for the same field as used by Maglich are presented, together with a discussion of their significance for beam injection and space-charge problems. In particular, our results show that inherent alternating-gradient effects increase the vertical focusing, but beyond a critical momentum value, the vertical oscillations become unstable because of overfocusing. Finally, some of the orbit data provided by Maglich are discussed and interpreted, along with his choice of magnetic field shape.

1. Introduction

In a recent article, Maglich has described the "Migma Cell", a potentially useful device for generating nuclear fusion power[1]). This device represents an extensive development of the "Migmatron", which is itself an outgrowth of the "Precetron"[2,3]). (These papers will hereafter be referred to collectively as Maglich et al.) The basic orbit properties of these devices, particularly the vertical focusing, have been treated rather casually using analytical methods based on the restrictive assumption of nearly circular orbits. A more rigorous treatment therefore seems desirable.

Precetron-Migma orbit properties can be accurately analysed using equilibrium orbits and transfer matrix techniques similar to those used in cyclic accelerators. The median-plane orbits execute a series of identical loops, going from r_{min} to r_{max} and back again to r_{min} in each loop. Although these orbits are generally not closed, the variation of the radius r is definitely periodic, and each orbit can therefore be viewed as an "equilibrium orbit" having a periodicity element equal to one loop. (The nonperiodicity of the azimuth θ is unimportant here since the field is axially symmetric.) With the equilibrium orbit thus defined, it becomes possible to calculate the transfer matrix for the vertical oscillations through one loop, and hence to determine the frequency v_z and other properties of these oscillations.

We have developed a computer code which, for a given median plane field $B(r)$, calculates all of the important properties of the equilibrium orbits and of the vertical oscillations as a function of the momentum p. The output from this code should make it possible

to evaluate rather quickly the advantages or disadvantages of a given field and operating condition. The structure of this code and some preliminary results are described in this paper.

In order to make the results as general as possible, we use a field unit B_0 and a length unit R_0, both of which are unspecified. All momenta are then expressed in terms of the unit:

$$p_0 = qB_0R_0/c, \tag{1}$$

for an ion of charge q. All of the results are then independent of the choice of a particular ion and of the "scale" of the device.

2. Equilibrium orbit (EO)

We use the arc length $s = vt$ as the independent variable, so that time never occurs explicitly in the results. In terms of cartesian coordinates, the differential equations for the EO are then given by:

$$dx/ds = p_x/p, \qquad dy/ds = p_y/p, \tag{2a}$$

$$dp_x/ds = -(p_y/p)B(r), \quad dp_y/ds = (p_x/p)B(r), \tag{2b}$$

where $B(r) = -B_z(r, z = 0)$, so that the ions rotate in the positive (counter-clockwise) sense.

The above equations are integrated numerically with the following initial conditions:

$$s = 0, \quad x = 0, \quad y = y_0, \quad p_x = p, \quad p_y = 0. \tag{3}$$

In addition to a given p, the orbit therefore has a specified value of $r_{min} = |y_0|$, and the sign of y_0 determines whether or not the orbit circles the origin. As the integration proceeds, the code calculates the

following polar variables:

$$r = (x^2 + y^2)^{\frac{1}{2}}, \qquad (4a)$$

$$p_r = (xp_x + yp_y)/r, \quad p_\theta = (xp_y - yp_x)/r. \qquad (4b)$$

The invariance of p^2 and of the generalized angular momentum (defined later) are used only to check the accuracy of the integration.

Because of the EO symmetry, only one-half of a loop is needed to completely specify all of the EO properties. The integration therefore runs from $s = 0$, where $r = r_{\min}$ only to the points $s = s_1$, where $r = r_{\max}$ and $p_r = 0$. Since the precise value of s_1 is unknown in advance, the code uses an iteration scheme to determine s_1 accurately. At the conclusion of this integration, the final conditions for this one-half loop are then given by:

$$s = s_1, \quad x = x_1, \quad y = y_1, \quad p_r = 0, \quad p_\theta = p. \qquad (5)$$

The value of $r_{\max}$ is then calculated from:

$$r_{\max} = (x_1^2 + y_1^2)^{\frac{1}{2}}. \qquad (6)$$

The above final conditions yield two additional important properties of the EO, namely, the "orbit radius" a, and the "precession fraction" f_p. The value of a is defined by and calculated from:

$$a = S/2\pi = s_1/\pi, \qquad (7)$$

where S is the total arc length of one loop, and hence the period of the EO. The precession fraction f_p is obtained from:

$$f_p = \theta_p/2\pi = (1/\pi)\tan^{-1}(-x_1/y_1), \qquad (8)$$

where the "precession angle" θ_p is the azimuthal displacement of the EO after each loop. That is, the momentum vector rotates through an angle $2\pi + \theta_p$ during each loop.

For a specified y_0 value, the code performs the above EO calculations for a sequence of p values: $p = \delta p$, $2\delta p$, $3\delta p$, ..., for a given δp interval. The code stops when a value $p = p_{\max}$ is reached such that the trajectory enters the region of negative field values. For a Precetron—Migma device, the orbits of primary interest are those which pass through or close to the origin, that is, those having $y_0 = 0$ or $y_0 \approx 0$.

The results described in this paper were obtained for the same field as that used by Maglich et al. In their notation, the median plane field is: $B_z = B_0(1 - kr^2/R^2)$. With B_0 as the field unit, and $R_0 = R$ as the length unit, this field becomes in our notation:

$$B(r) = 1 - kr^2, \qquad (9)$$

with the momentum unit of eq. (1) given by: $p_0 = qB_0R/c$. Although we explicitly maintain the field index k as a parameter, the results obtained for different k values are related quite simply. To show this, we need merely point out that if we had chosen the length unit $R_0 = R/\sqrt{k}$, and the momentum unit $p_0 = qB_0R/(c\sqrt{k})$, then our median-plane field would have been: $B(r) = 1 - r^2$, independent of k. In order to emphasize the k dependence, the results displayed in our figures contain the scale factor $\sqrt{k}$ for lengths and momenta. Only the results obtained for $y_0 = 0$ will be presented and discussed in detail.

Before presenting our EO results, we should point out some important conclusions which can be drawn from the invariance of the generalized angular momentum K given by:

$$K = rp_\theta - \int rB(r)\,dr, \qquad (10)$$

which uniquely specifies p_θ as a function of r. For example, in the case where $y_0 = 0$, if the initial and final conditions of eqs. (3) and (5) are inserted, we obtain:

$$pr_1 = \int rB(r)\,dr, \qquad (11)$$

where the integration here runs from $r = 0$ to $r = r_1 = r_{\max}$. This result then provides a definite relationship between r_1 and p.

For the field under consideration with $B(r)$ given by eq. (9), we find:

$$p = \tfrac{1}{2}r_1(1 - \tfrac{1}{2}kr_1^2). \qquad (12)$$

In particular, this equation shows that there is some momentum value P such that for $p > P$, no solution for r_1 exists. The value $p = P$ therefore represents the maximum momentum which the field can "confine" for the given $y_0 = 0$ value. Setting $dp/dr = 0$ at $r = R_1$, we then obtain:

$$R_1 = \sqrt{(\tfrac{2}{3}k)} = 0.816/\sqrt{k}, \qquad (13a)$$

$$P = \tfrac{1}{3}R_1 = 0.272/\sqrt{k}. \qquad (13b)$$

Thus, all orbits with $y_0 = 0$ and having $p < P$ will lie inside the circle $r = R_1$. A half loop for three such orbits is shown in fig. 1 for $p\sqrt{k} = 0.134, 0.201,$ and 0.271.

Since the value $r = R_1$ and $p = P$ given above satisfy the condition for a circular orbit: $p = rB(r) = r(1 - kr^2)$, we must conclude that the orbit which starts from the center with $p = P$ spirals outward and around the origin approaching the circle $r = R_1$ asymptotically.
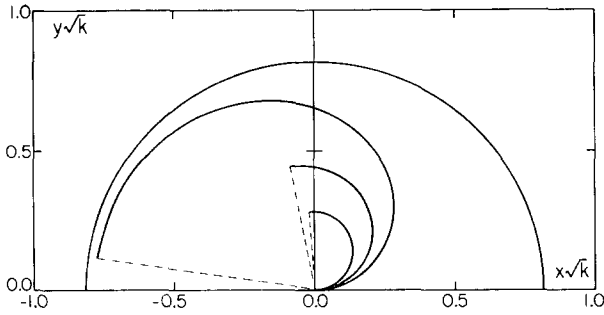
Fig. 1. XY plots of three median-plane (equilibrium) orbits having momenta: $p\sqrt{k} = 0.134$, 0.201, and 0.271. These half loops start at $r = 0$, $\theta = 0$, and end (as indicated by broken line) at $r = r_{max}$, $\theta = \frac{1}{2}(\pi + \theta_p)$, where θ_p is the "precession angle". Lengths are in units of R, momenta in units of $qB_0 R/c$, and the scale factor $\sqrt{k}$ shows the dependence on the field index k. Circle at $r = 0.816/\sqrt{k}$ indicates limiting value of r_{max} for "confined" orbits.

This implies that as p approaches P, the orbit radius a of eq. (7) and the precession fraction f_p of eq. (8) will both approach infinity. This behavior is indicated to a certain extent by the orbits in fig. 1.

The approximation assuming nearly circular orbits used by Maglich et al. yields the equation $a = p$ for the orbit radius when expressed in our units. The computer results show that a increases faster than p, and approaches infinity for $p \to P$, as expected. The approximation $a = p$ is valid only for $p < 0.15/\sqrt{k}$.

Fig. 2 shows a plot of the precession fraction f_p as a function of $p\sqrt{k}$ as derived from the computer output. When translated into our units, the analysis of Maglich et al. yields the relation: $f_p = kp^2$, which is
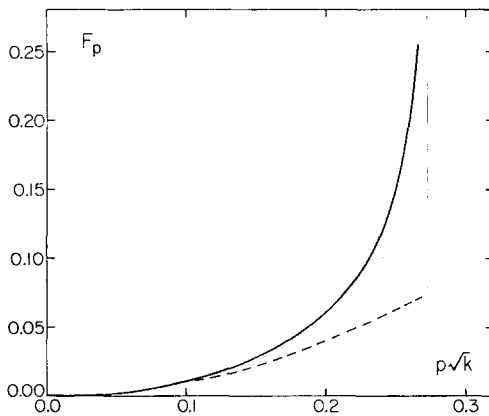

Fig. 2. Plot of precession fraction $f_p = \theta_p/2\pi$ vs $p\sqrt{k} = (mvc/qB_0 R)\sqrt{k}$. Broken curve shows approximation: $f_p = kp^2$. Vertical line at $p = 0.272/\sqrt{k}$ indicates maximum momentum for "confined" orbits.

shown as a broken curve in fig. 2. This approximation is evidently valid for small values of $p\sqrt{k}$, but the actual f_p curve rises faster than kp^2, and approaches infinity for $p \to P$, as noted above.

Whenever $f_p = \theta_p/2\pi$ is a simple rational fraction, the median plane orbit will close on itself after a small number of loops. Such orbits must be avoided for the injection of primary Migma ions, or else they will return to strike the inflector before they can be "self-ensnared", as described by Maglich[1]. To avoid this difficulty, quite small values of f_p would be most advantageous. That is, when f_p is quite small, the number of loops required for the ion to return to the inflector is approximately $1/f_p$. However, if f_p is too small, the ions will return to strike an inflector of finite size after only one loop.

3. Vertical focusing

For orbits such as those shown in fig. 1, the field gradient is evidently stronger near $r = r_{max}$ than near $r = 0$, so that the vertical focusing has a significant alternating-gradient (AG) component. Since the EO is periodic with period $S = 2\pi a$, we expect the vertical oscillations to have the same form as in AG accelerators, namely:

$$z(s) = W(s) \cos[v_z(s/a) + \psi(s)]. \quad (14)$$

Here, v_z is the frequency in oscillations per loop, and both $W(s)$ and $\psi(s)$ are periodic with the same period S. The "form factor" $W(s)$, in combination with $r(s)$ for the EO, can be used to obtain the vertical distribution of Migma ions as a function of radius. In this section, we describe how the code computes v_z and $W(s)$.

The differential equations for the vertical oscillations are given by:

$$dz/ds = p_z/p, \quad (15a)$$

$$dp_z/ds = [(p_\theta/p)(dB/dr)]z, \quad (15b)$$

where the quantity in brackets is evaluated on the EO at each s value. In order to construct the transfer matrix, the code generates two solutions (z_1, p_{z1}) and (z_2, p_{z2}), with initial conditions $(1,0)$ and $(0,1)$, respectively. These integrations are carried out from $s = 0$ to $s = s_1$ simultaneously with the final integration of the EO described above.

Because $r(s)$ for the EO is symmetric about the two points $s = 0$ and $s = s_1$, only the transfer matrix for one half of a loop $(0 < s < s_1)$ is required to produce the complete transfer matrix. From an analysis of a comparable situation presented in a previous paper,

we have the following equations for calculating v_z and the parameter β_0 [4]):

$$\cos(2\pi v_z) = z_1(s_1)\, p_{z2}(s_1) + z_2(s_1)\, p_{z1}(s_1), \qquad (16a)$$

$$\sin(2\pi v_z) = (2/\beta_0)\, z_2(s_1)\, p_{z2}(s_1)$$

$$= -(2\beta_0)\, z_1(s_1)\, p_{z1}(s_1). \qquad (16b)$$

The code uses these equations to obtain β_0 and v_z.

The form factor $W(s) = \sqrt{\beta(s)}$ can be calculated from the equation:

$$W^2(s) = \beta(s) = \beta_0 z_1^2(s) + (1/\beta_0)\, z_2^2(s), \qquad (17)$$

with $\beta_0 = \beta(s = 0)$ given above. This $W(s)$ is symmetric about the points $s = 0$ and $s = s_1$. Moreover, $W(s)$ has its minimum value $W_0 = \sqrt{\beta_0}$ at $s = 0$, and its maximum value $W_1 = \sqrt{\beta_1}$ at $s = s_1$. In particular, the important ratio W_0/W_1 is given by:

$$(W_0/W_1)^2 = \beta_0/\beta_1 = p_{z2}(s_1)/z_1(s_1). \qquad (18)$$

In addition to v_z, the code prints out values of W_0 and W_1 as a function of p.

Fig. 3 shows a plot of v_z versus $p\sqrt{k}$ for EO's starting at $r = 0$, some of whose other properties are shown in figs. 1 and 2. When translated into our units, the analysis of Maglich et al. yields the result: $v_z = p\sqrt{/(2k)}$, which is shown by the broken line in fig. 3. This approximation is (once again) valid only for small values of $p\sqrt{k}$.

The v_z curve in fig. 3 rises faster than $p\sqrt{/(2k)}$, and reaches the critical value $v_z = \frac{1}{2}$ at $p = 0.215/\sqrt{k}$. Above this p value, the vertical oscillations become unstable as a result of "over-focusing". In this over-focusing region ("π stop-band"), which extends from $p = 0.215/\sqrt{k}$ to $p = 0.253/\sqrt{k}$, the values of v_z are complex and given by:

$$v_z = \frac{1}{2} \pm i v_z^*. \qquad (19)$$

The code also provides the values of v_z^* where appropriate, and these are plotted at the top of fig. 3. Although the values shown for $v_z^*(<0.11)$ may appear small, they are actually quite substantial. To grasp this, it should be recognized that the vertical oscillation amplitude will (eventually) grow by a factor $\exp(2\pi v_z^*)$ on each loop.

Fig. 4 shows the values of the ratio W_0/W_1 plotted against $p\sqrt{k}$ in the region of vertical stability, $p < 0.215/\sqrt{k}$. For $p \approx 0$, $W(s)$ is nearly constant, so that $W_0/W_1 \approx 1$. The values of W_0/W_1 shown in fig. 4 fall slowly at first with increasing $p\sqrt{k}$, and then drop sharply to 0 as the critical value $p\sqrt{k} = 0.215$ is approached. Given the choice, a low value of W_0/W_1 would be most desirable, since such a value would produce a higher density in the central core of the Migma.

For the sake of clarity, fig. 3 does not show the rapid changes in v_z which occur in the small range between $p = 0.253/\sqrt{k}$ and $p = 0.272/\sqrt{k}$, the maximum possible p value. First, from $p = 0.253/\sqrt{k}$ to $p = 0.268/\sqrt{k}$, the value of v_z becomes real again and rises from $v_z = \frac{1}{2}$ to $v_z = 1$. Then, in the remaining narrow range of p values, the value of v_z passes through at least two additional regions of instability (the 2π and 3π stop-bands). Since the Migma ions must have a distribution of p values, it would therefore be rather dangerous to operate anywhere except in the primary region of stability, $p < 0.215/\sqrt{k}$.
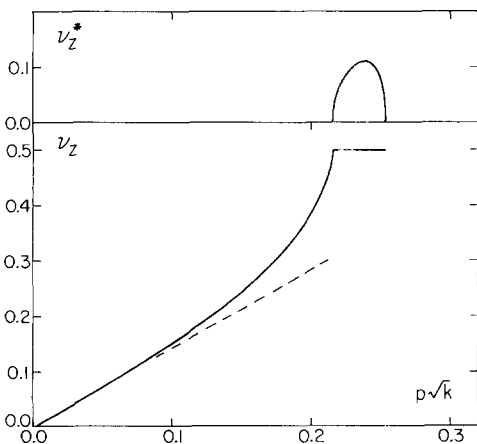
Fig. 3. Plot of frequency v_z (vertical oscillations per loop) vs momentum variable $p\sqrt{k}$. Lower curve shows real part of v_z, while upper curve shows imaginary part v_z^*. Vertical lines indicate region of instability from $p\sqrt{k} = 0.215$ to 0.253. Broken line shows approximation: $v_z = p\sqrt{/(2k)}$.
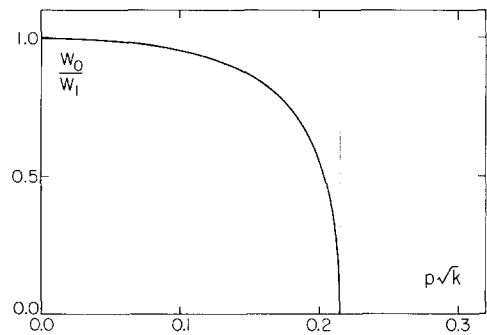
Fig. 4. Plot of ratio W_0/W_1 of minimum to maximum amplitude of vertical oscillations as a function of the momentum variable $p\sqrt{k}$ within the region of stability, $p\sqrt{k} < 0.215$. Minimum amplitude W_0 occurs at $r = 0$, while maximum amplitude W_1 occurs at $r = r_{max}$.

Any median plane orbit which starts at $r = 0$ returns exactly to that point after one loop. In this case, the frequency of the horizontal oscillations about the given EO must have the value: $v_r = 1$.

All of the results discussed above were obtained for EO's which start at $r = 0 (y_0 = 0)$. Comparable data have also been obtained for the cases where $y_0 = \pm 0.01/\sqrt{k}$. As expected, for positive (negative) value of y_0, the values of v_z are larger (smaller) than those for $y_0 = 0$. However, for the y_0 values considered, these differences are not large enough to be significant.

4. Summary and conclusions

For the median plane field used by Maglich et al. $B_z = B_0(1 - kr^2/R^2)$, all of the orbit properties depend on the field index k only through a scale factor $\sqrt{k}$ for lengths and momenta. This scaling property is indicated in our figures where we use the momentum variable $p\sqrt{k} = (mvc/qB_0 R)\sqrt{k}$. We have found that the approximate formulas used by Maglich et al. for the orbit radius a, for the precession fraction f_p, and for the vertical oscillation frequency v_z, are generally valid only for $p\sqrt{k} < 0.15$.

In order to maximize the space charge limit, it would be advantageous to have v_z as large as possible. However, to avoid vertical instability through overfocusing, the value of v_z must be restricted to the range: $v_z < 0.5$, which (as shown in fig. 3) requires $p\sqrt{k} < 0.215$ for this particular field. Moreover, it should be noted that the behavior of v_z versus p will be qualitatively the same for any field which is suitable to a Precetron-Migma device.

As discussed at the end of sect. 2, the injection of primary Migma ions would be facilitated if the precession fraction f_p (shown in fig. 2) is as small as possible. However, our data show that the formula:

$$v_z = \sqrt{(2f_p)}, \tag{20}$$

is a good approximation for $f_p < 1/25$ or $v_z < 0.3$. Thus, lower f_p values will always coincide with lower v_z values which, as indicated above, are undesirable. A possible solution to this dilemma might be achieved by injecting the ions off the median plane under conditions where the precession period and the vertical oscillation period combine in such a way as to provide a much longer time before the ions return to strike the inflector. Maglich apparently proposes such a scheme in his discussion of the injection process[1]).

In his design of the "Migma Cell", Maglich uses 2.2 MeV deuterons in a field characterized by

$B_0 = 200$ kG, $k = 0.8$, and $R \approx 5$ cm[1]). Together with a 4% energy spread, these parameters imply: $p\sqrt{k} \approx 0.27 \pm 0.003 > 0.215$, so that according to our data, the resultant orbits will lie in the region of vertical instability. It should be kept in mind, however, that the effect of this "instability" is not unlimited provided sufficient space is available for the resultant large amplitude vertical oscillations. Since the horizontal oscillation frequency has the value $v_r = 1$, then for $v_z \approx 0.5$, these vertical oscillations will come under the influence of the $v_r = 2v_z$ nonlinear coupling resonance. This resonance commonly occurs in the extraction region of most cyclotrons, and its properties are well known[5]). It is characterized by a (conservative) back and forth interchange of energy between the vertical and horizontal oscillations. In this situation, the focusing is centered not on a median plane EO, but rather on a three-dimensional periodic "fixed-point" orbit which resembles a "figure 8" bent at the middle and nearly doubled over. Unfortunately, Maglich does not supply sufficient data on the orbits of the 2.2 MeV deuterons for us to reach more definite conclusions.

The only specific orbit data furnished by Maglich appears in his fig. 2 and fig. 3 which show orbits of ions scattered (or injected) at $r = z = 0$ with different angles θ_z relative to the median plane[1]). Although these orbits relate to other energies and different fields, they display some interesting properties. The orbit in his fig. 2 with $\theta_z = 10°$ can be recognized as one which executes a small oscillation about the fixed-point orbit of the $v_r = 2v_z$ resonance discussed above. Also, the orbit shown in fig. 3 with $\theta_z = 40°$ resembles the fixed-point orbit associated with the higher order $v_r = 6v_z$ coupling resonance. Ions moving in such orbits would spend relatively little time near the median plane. Maglich does not show in these figures any orbits for very small θ_z values, but judging from the given data, we conclude that such orbits would be "unstable". That is, these orbits would remain close to the median plane only for a short time, and under the action of the nonlinear coupling resonance, the amplitude of the vertical oscillations would then grow rapidly and reach a very large value before declining again. Considering these complications, a more systematic investigation should be carried out in order to establish the desirability and the consequences of operating a Migma device under the strong action of nonlinear coupling resonances.

The orbit computations presented by Maglich et al. (and by us in this paper) are based on a specially chosen magnetic field shape which they have success-

fully fitted using two (or three) pairs of coils[1]). This special field contains terms only to order r^2 and z^2, and has the property that curl $B = 0$ everywhere, so that its sources are nominally located at infinity. Such a fiield should not be used for orbit computations unless these orbits have a radial and vertical extent which is negligible compared to that of the coils. In particular, this simple field cannot be expected to provide very reliable information on nonlinear coupling resonances. Furthermore, our results suggest that *any* axially symmetric field $B_z(r, z)$ which, in the median plane, falls off with increasing radius will produce the basic orbit precession and vertical focusing required for a Migma device. The design of an optimum coil configuration should therefore be based on more practical considerations.

Note added in proof (9/74): Further calculations, which include all nonlinear effects, have confirmed the inferences made above regarding the action of nonlinear coupling resonances in controlling the behavior of large-amplitude vertical oscillations. A detailed report on these calculations will be submitted for publication soon.

References

[1] B. Maglich, Nucl. Instr. and Meth. **111** (1973) 213; brief reports of more recent work can be found in: Bull. Am. Phys. Soc. **18** (1973) 556, 1322; Bull. Am. Phys. Soc. **19** (1974) 62.

[2] B. C. Maglich, J. P. Blewitt, A. P. Colleraine and W. C. Harrison, Phys. Rev. Lett. **27** (1971) 909.

[3] R. Macek and B. Maglich, Particle Accellerators **1** (1970) 121; R. E. Knop and A. P. Colleraine, Particle Accellerators **2** (1971) 301.

[4] M. M. Gordon, Ann. Phys. **50** (1968) 571.

[5] W. Joho, 5th Intern. Cyclotron Conf. (Butterworths, London, 1971) p. 159.